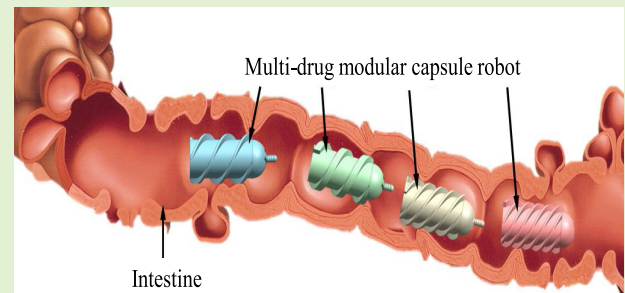


Multimodular Capsule Robot System With Drug Release for Intestinal Treatment

Lingling Zheng^{ID}, Shuxiang Guo^{ID}, *Fellow, IEEE*, and Masahiko Kawanishi, *Member, IEEE*

Abstract—Capsule robots have the potential for intestinal treatment due to their unique advantages compared with traditional diagnosis and treatment. However, current capsule robots can only carry and release one type of drug, while more drugs would be needed during the treatment. In addition, the volume of loaded drugs will be restricted due to the small dimensions of the capsule robot, and released drugs need to be guaranteed to have a sufficient dosage for treatment. In this article, to overcome these limitations, a system was proposed, and the robot consists of a leader robot module and several robot modules. Each robot module can load two types of drugs, and any two robot modules can achieve docking and separations according to the clinical requirements. Laboratory experiments were carried out to evaluate the performance. The experimental results show that the robot modules can move with speeds of 28.5, 25.1, 22.3, and 14.5 mm/s when they load drugs of 0, 0.6, 1.2, and 1.8 g, respectively. Ex vivo experiments demonstrated that two robot modules could dock and separate from each other and release drugs at target positions and did not cause damage to the lining of the intestine. This proposed multidrug modular capsule robot could prove a reference for drug release and control and have the potential for further applications.

Index Terms—Capsule robot, intestinal treatment, magnetically controlled robot, multiply drug releases.



I. INTRODUCTION

SMALL intestine disease is an ever-increasing clinical problem threatening people's health since more people adopt unhealthy lifestyle habits [1], [2]. The small intestine is located in the middle of the digestive tract, close to 7 m long and far away from the mouth and anus, so it is difficult to observe and diagnose [3]. However, with the advancement of

Manuscript received 9 September 2022; revised 23 January 2023; accepted 6 April 2023. Date of publication 12 July 2023; date of current version 15 August 2023. This work was supported in part by the National High-Tech Research and Development Program (863 Program) of China under Grant 2015AA043202; in part by the Research Foundation of Nanjing Xiaozhuang University under Grant 2022NXY08; in part by the Natural Science Foundation of the Jiangsu Higher Education Institutions of China under Grant 23KJB460023; and in part by the Natural Science Foundation of Jiangsu Province. The associate editor coordinating the review of this article and approving it for publication was Dr. Ali Mohammadi. (*Corresponding author: Shuxiang Guo.*)

Lingling Zheng is with the School of Information Engineering and the School of Artificial Intelligence, Nanjing Xiaozhuang University, Nanjing 211171, China (e-mail: zhenglingling2018@outlook.com).

Shuxiang Guo is with the Department of Electronic and Electrical Engineering, Southern University of Science and Technology, Shenzhen 518055, China, and also with the Key Laboratory of Convergence Medical Engineering System and Healthcare Technology, Ministry of Industry and Information Technology, Beijing Institute of Technology, Beijing 100081, China (e-mail: guo.shuxiang@sustech.edu.cn).

Masahiko Kawanishi is with the Faculty of Medicine, Kagawa University, Takamatsu 761-0793, Japan (e-mail: mk@kms.ac.jp).

Digital Object Identifier 10.1109/JSEN.2023.3281579

endoscopy equipment and technology, significant progress has been made in diagnosing and treating small intestine diseases.

Nowadays, capsule endoscopy and enteroscopy are common medical processes for diagnosing and managing small intestine disorders, and these two technologies can be used alone or in combination [4]. By combining these two technologies, capsule endoscopes can provide preliminary detection image information, which can help enteroscopy confirm the lesions' position to perform further treatment procedures [5]. However, some problems still need to be solved in the clinical procedure by using capsule endoscopy and enteroscopy to diagnose and treat small intestine diseases. First, the capsule endoscope is limited by its volume, making it hard to add other functions besides image collection and transmission. Second, colonoscopy has the risk of complications and perforation, and the implementation process will bring discomfort to the patient. Third, if two technologies are used simultaneously, medical procedures will become complicated, and their functions have part of overlap. It wastes medical resources and increases the financial burden of patients. Therefore, many research groups focus on developing functional capsule robots to combine capsule endoscopy and enteroscopy advantages.

Active locomotion or anchoring is one of the essential functions of the capsule robot design that allows the position to be controlled when the capsule robot travels in the intestine [6], [7]. It helps the capsule robot adjust the

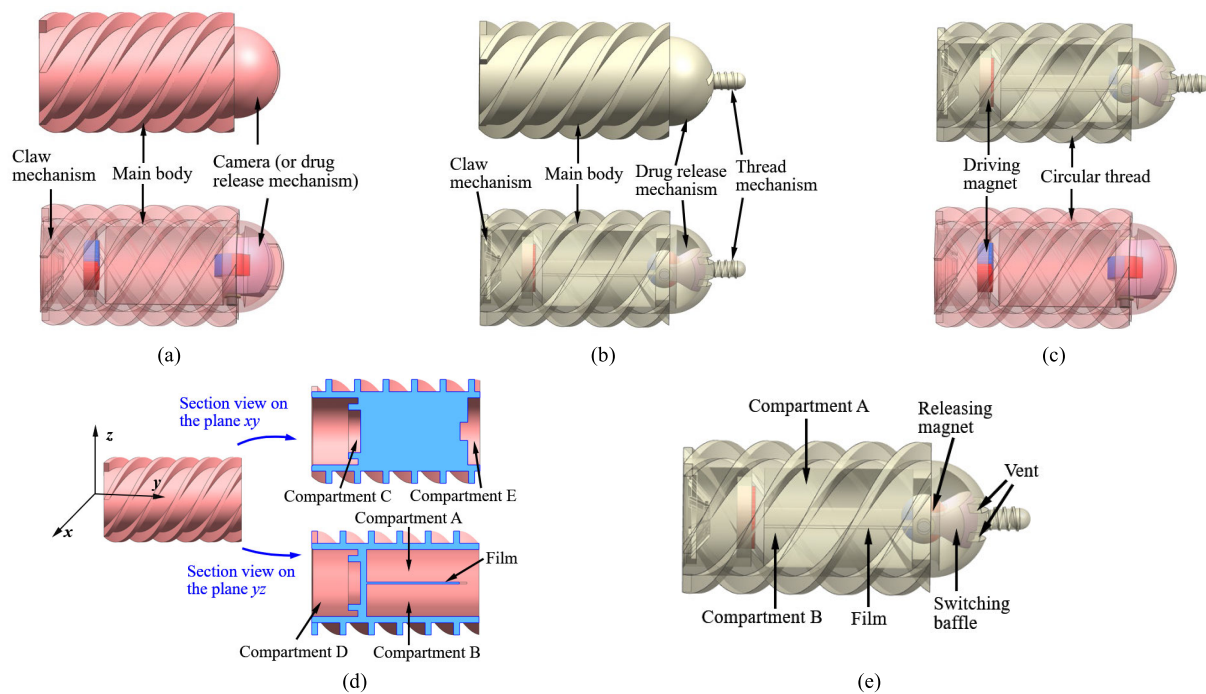


Fig. 1. Design details of multidrug modular capsule robot modules. (a) Leader robot module. (b) Follower robot module. (c) Driving mechanism. (d) Internal structure of the main body. (e) Drug release mechanism.

field of view as desired and stay around a specific location to increase inspection accuracy [8]. In addition, drug delivery is one of the basic treatment functions of the capsule robot design during intestinal disease surgery [9], [10]. Therefore, many multifunctional capsule robots with active locomotion and drug delivery have been developed [11], [12], [13], [14], [15]. Nam et al. [12] proposed a magnetic helical robot that can release a drug to a targeted area and perform an active movement in tubular environments of the human body. Munoz et al. [13] presented a capsule robot manipulated by the external magnetic system made of an array of 24 arch-shaped permanent magnets. This capsule robot can achieve targeted drug delivery through an onboard drug release mechanism that can be actuated at any position. Nguyen et al. [14] proposed a robotic capsule endoscope with a delivery module that can actively move to the target region to treat digestive diseases. Song et al. [15] proposed a novel capsule robot that magnetically actuated anchoring and drug release in the lower gastrointestinal (GI) tract. In previous research, we have developed a series of capsule robots to achieve active movement and drug delivery functions [16], [17], [18], [19], [20]. Guo et al. [16] presented a push-type capsule robot equipped with a piston, spring, drug compartment, and magnetic lock. The magnetic lock of the robot can be released; then, the piston is squeezed out of the drug chamber by the combination of the spring force and the attraction of the magnet. Guo et al. [17] designed a robot module, and Wang et al. [18], [19] proposed a drug-sustained release minirobot (DSM) to spray the medicine in the medicine warehouse to the designated position. The robots equipped two radially magnetized magnets rotating along the thin rod and used the repulsive or attraction force between the magnets to squeeze the medicine from the drug

delivery port. All the above capsule robots can only carry and release one type of drug, while more drugs would be needed during the treatment. Moreover, released drugs need to be guaranteed to have a sufficient dosage for treatment, which brings a requirement on the volume of drugs loaded by capsules. Hence, capsule robots are required to be equipped with more types and quantities of loaded drugs. These problems introduce application restrictions for capsule robots.

In this article, to overcome the limitations mentioned above, we propose a multidrug modular capsule robot system. The multidrug modular capsule robot system consists of several capsule robot modules, as shown in Fig. 1, and these modules have independent functions and cooperation. The proposed module is able to load two types of drugs and achieve docking and separation with the other modules. Compared to the previous studies, the proposed multidrug modular capsule robot system has the following advantages. The multimodular capsule robot system provides a new method for expanding the inspection and treatment functions of the capsule endoscope. The proposed capsule modules have multifunction, including active movement, drug delivery, docking, and separation. Munoz et al. [13] and Nguyen et al. [14] move through the intestinal tract in the passive mode under the gastrointestinal peristalsis and Song et al. [15], Guo et al. [16], [17], and Wang et al. [18], [19] did not equip with multifunctional mechanisms besides the drug release and active movement mechanism. Moreover, the system can carry multiple drugs to the target location, and each module is able to take two types of drugs. By increasing the number of modules of the system, the limitation of the drug's amount and types can be broken through. Nam et al. [12], Munoz et al. [13], Nguyen et al. [14], Song et al. [15], Guo et al. [16], [17], and

Wang et al. [18], [19] proposed that capsule robot can only release one kind of drug, and the dose is limited by its size.

This article is organized as follows. Section II presents the methodology of the proposed multidrug modular capsule robot system, including workflow, design details, mechanical analysis and control, and prototype. Experiments evaluating the performance of the proposed system, including locomotion, docking and separation, and drug delivery, are detailed in Section III. Section IV describes the ex vivo experiments. The conclusion and future work are summarized in Section V.

II. METHODOLOGY

A. Workflow

As shown in the Abstract, the multidrug modular capsule robot consists of several capsule robot modules and the robot modules can move along the intestine with the control of the magnetic field. They move to the target position that needs to be treated and then released drugs. Since various drugs are required for some treatments, different robot modules will be controlled to release various drugs or more dosages at the target position. When more robot modules are used, navigating them one by one to the target position will increase the treatment difficulty and time. Thus, these robot modules are designed to be able to dock and separate with each other according to the requirements. Based on this design concept, one robot module is employed as the leader robot module, and the other robot modules work as the follower robot modules. The leader robot module can be potentially equipped with cameras that can capture images of the intestine interior. With captured images, the operators can see the internal intestinal conditions and adjust the movement speed and direction of the robot modules, thus improving the navigation efficiency and accuracy. The leader robot module is the basic module for navigation and preliminary treatment; the follower robot modules are used to load various drugs for further treatment.

B. Design

As shown in Fig. 1(a) and (b), the leader robot module consists of a claw mechanism, main body, and camera. Since the camera needs to be powered wirelessly and we have not conducted the wireless power supply technology, in this research, we integrate the drug release mechanism into the leader robot module. Based on the design concept, cameras can be set in the leader robot module to replace the drug release mechanism in future work. The follower robot module comprises a claw mechanism, main body, drug release mechanism, and thread mechanism. The main body has circular threads on its surface. The circular threads and the driving magnet work together as a moving mechanism [see Fig. 1(c)]. The driving magnet drives the main body to rotate when an external magnetic field is applied. With the rotation of the circular threads, the robot module can move forward or backward. The moving mechanism provides the propulsive force and enables the robot module to move to the target position.

Fig. 1(d) shows the internal structure of the main body, including section views along the planes xy and yz . The main body consists of five compartments. Compartments A and

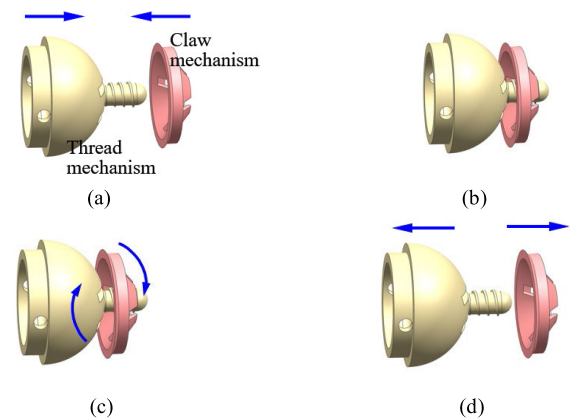


Fig. 2. Docking and separation. (a) Two robot modules move toward each other, (b) with the decrease of the distance, the thread mechanism enters the claw mechanism and completes the docking, (c) in order to achieve the separation, two robot modules rotate in opposite directions, and (d) after separation, two robot modules move separately.

B, used to load various drugs, are separated by the film. The driving magnet that can rotate the main body is set in compartment C. Compartments D and E are designed to install the claw mechanism and the drug release mechanism, respectively. The main body provides a platform and integrates all the mechanisms into a whole robot module.

As shown in Fig. 1(e), the drug delivery mechanism is composed of a releasing magnet and switching baffle. The position of the switching baffle can be changed by the rotation of the releasing magnet. The end cover has two vents that form different working statuses with the switching baffle. When the switching baffle moves to the upper limit position, the upper vent is sealed and the lower vent is open. At this time, the drug can be released from the lower vent. When the switching baffle moves to the lower limit position, the lower vent is sealed and the upper vent is open. At this time, the drug can be released from the upper vent. Different vents connect various compartments that load various drugs, and thus various drugs can be selected and released. When the switching baffle is located in the middle position, two vents are all sealed and no drugs will be released. Therefore, the drug delivery mechanism can release various drugs at desired targets according to the clinical requirements.

The claw mechanism has four claws that are arranged in a ring and form a hole in the center. The hole has threads and can engage with the thread mechanism. Fig. 2 shows the process of docking and separation. In order to achieve the docking, two robot modules move toward each other. The thread mechanism can enter the claw mechanism because the propulsive force makes the claws move outward. These two mechanisms cannot separate due to the characteristic of the annular claws. To achieve the separation, these two robot modules rotate in opposite directions and then the thread mechanism turns out of the claw mechanism. Moreover, the proposed docking and separation mechanism can help the capsule robot system move in a curved path. The docking and separation mechanism uses the engagement of the claw mechanism and thread mechanism to provide the docking force. The angle formed by the docking robot modules can be adjusted by modifying the radius of

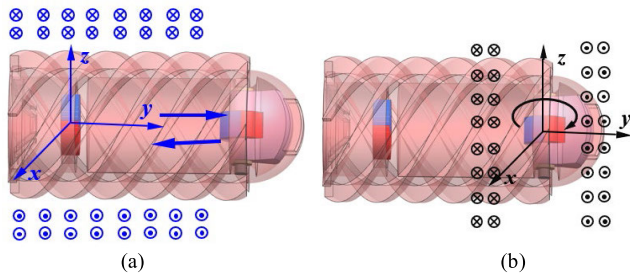


Fig. 3. (a) Robot module performs locomotion with the rotating magnetic field around y -direction. (b) Releases drugs with the rotating magnetic field around the z -direction.

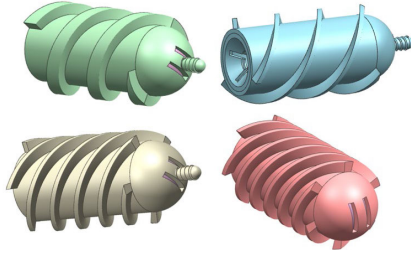


Fig. 4. Various types of robot modules with different step-out frequencies.

curvature in the thread mechanism. The docking modules will have an angle with the central axis, which helps them pass through the curved intestinal tract. The calculation and modeling of the turning angle are introduced in [22].

C. Locomotion and Drug Release Control

The multidrug modular capsule robot is remotely controlled by the external magnetic field, and when various external magnetic fields apply, the multidrug modular capsule robot can achieve different working states. As shown in Fig. 3(a), in order to achieve locomotion of the robot module, a rotating magnetic field around the axial direction of the robot module (y -direction) is generated, and then the robot module will rotate and move since the driving magnet in the main body of the robot module is subjected to the rotational force with the rotating magnetic field. However, when multiple robot modules are used simultaneously, there will be a challenge for this control method because magnets in other robot modules will also be applied with the rotational force when robot modules move in the intestine close to each other and the axes of the robot modules are almost in a straight line, as shown in the Abstract To address this challenge, we developed the robot module with various weights and structures, as shown in Fig. 4. These robot modules have different thread structures, thread numbers, and thread angles, which result in various moments of inertia. Therefore, these robot modules have different step-out frequencies that allow the robot modules to be controlled separately [21], [22]. When the applied magnetic field rotates slowly, the microrobots synchronously rotate with the field. When the magnetic control robot is operated above one frequency (the frequency requiring the entire available magnetic torque to maintain synchronous rotation),

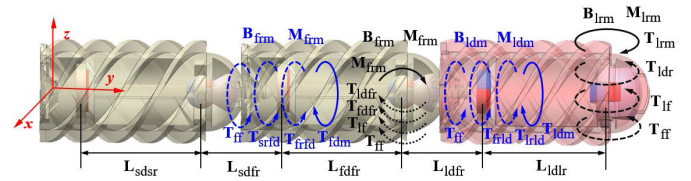


Fig. 5. Schematic of mechanical analysis.

the velocity of the robot dramatically declines. This frequency is the “step-out” frequency.

To achieve the drug release, a rotating magnetic field around the z -direction is generated and applied to the releasing magnet. The releasing magnet drives the switching baffle to rotate and then one drug will be released from the vent [see Fig. 3(b)]. However, similar to the locomotion control of multiple robot modules, the releasing magnets in various robot modules will interfere with each other in the same rotating magnetic field. To address this issue, we propose installing the driving magnets with different phase angles relative to the axes of the releasing magnets. With this method, when one drug release mechanism needs to be controlled, a constant magnetic field, for example, around the x -direction, is generated, and all the robot modules will rotate at a special angle, thus resulting in all the releasing magnets with various angles relative to the z -direction. Based on the various angles relative to the z -direction, drug release mechanisms can be controlled separately by using rotating magnetic fields around various directions.

D. Mechanical Analysis

In order to control the drug release mechanism in the leader robot module, a rotating magnetic field is applied to the releasing magnet and the releasing magnet can provide a driving torque for the drug mechanism. During the drug release, the driving magnet in the leader robot module will exert a force on the releasing robot since they are permanent magnets that produce magnetic fields. In addition, the resistance torques generated by the film and frictions will also apply to the releasing magnet. Therefore, the resultant torque applied to the releasing magnet in the leader robot module can be expressed as (see Fig. 5)

$$\mathbf{T}_{lr} = \mathbf{T}_{lrm} - \mathbf{T}_{ldr} - \mathbf{T}_{lfr} - \mathbf{T}_{lff} \quad (1)$$

where \mathbf{T}_{lrm} is the torque exerted on the releasing magnet in the leader robot module by the rotating magnetic field, \mathbf{T}_{ldr} means the resistance torque generated by the interaction between the driving magnet and the releasing magnet in the leader robot module, \mathbf{T}_{lfr} indicates the resistance torque generated by the film, and \mathbf{T}_{lff} is the resistance torque generated by the frictions. In this research, the bold parameters are 3-D vectors since all the robot modules move in the intestine with 3-D shapes. The torque exerted on the releasing magnet by the rotating magnetic field can be obtained by

$$\mathbf{T}_{lrm} = V_{lrm} \mathbf{M}_{lrm} \times \mathbf{B}_{lrm} \quad (2)$$

where V_{lrm} is the volume of the releasing magnet in the leader robot module, \mathbf{M}_{lrm} is the magnetization of the releasing

magnet in the leader robot module, and \mathbf{B}_{lrm} means the magnetic flux density of the rotating magnetic field applied to the releasing magnet in the leader robot module. The resistance torque generated by the interaction between the driving magnet and the releasing magnet in the leader robot module can be written as

$$\mathbf{T}_{ldr} = AL_{ldr}^{-3} \mathbf{M}_{ldm} \times \mathbf{M}_{lrm} + 3AL_{ldr}^{-5} \mathbf{M}_{lrm} \times \mathbf{L}_{ldr} (\mathbf{M}_{ldm} \cdot \mathbf{L}_{ldr}) \quad (3)$$

where A is a constant and equals $\mu_0/4\pi$, in which μ_0 means the permeability of the air, \mathbf{M}_{ldm} is the magnetization of the driving magnet in the leader robot module, and \mathbf{L}_{ldr} represents the distance between the driving magnet in the leader robot module and the releasing magnet in the leader robot module. Actually, the releasing magnet in the leader robot module also interacts with the driving/releasing magnets in both the follower robot module and the second-follower robot module. We did not give the equations indicating these resistance torques in this research since they are small, but they can be obtained by referencing (3) for further consideration. The equations indicating these small resistance torques were also omitted in the following analysis.

When a rotating magnetic field is applied to the driving magnet in the leader robot module, the driving magnet overcomes resistance torques and rotates to achieve locomotion. The resultant torque applied to the driving magnet in the leader robot module is

$$\mathbf{T}_{ld} = \mathbf{T}_{ldm} - \mathbf{T}_{lrld} - \mathbf{T}_{frld} - \mathbf{T}_{ff} \quad (4)$$

where \mathbf{T}_{ldm} is the torque exerted on the driving magnet in the leader robot module by the rotating magnetic field, \mathbf{T}_{lrld} means the resistance torque generated by the interaction between the releasing magnet and driving magnet in the leader robot module, and \mathbf{T}_{frld} means the resistance torque generated by the interaction between the releasing magnet in the follower robot module and the driving magnet in the leader robot module. The torque exerted on the driving magnet in the leader robot module by the rotating magnetic field can be expressed as

$$\mathbf{T}_{ldm} = V_{ldm} \mathbf{M}_{ldm} \times \mathbf{B}_{ldm} \quad (5)$$

where V_{ldm} is the volume of the driving magnet in the leader robot module and \mathbf{B}_{ldm} means the magnetic flux density of the rotating magnetic field applied to the driving magnet in the leader robot module. Similarly, the resistance torques generated by the interaction between two magnets can be obtained by

$$\mathbf{T}_{lrld} = AL_{ldr}^{-3} \mathbf{M}_{lrm} \times \mathbf{M}_{ldm} + 3AL_{ldr}^{-5} \mathbf{M}_{ldm} \times \mathbf{L}_{ldr} (\mathbf{M}_{lrm} \cdot \mathbf{L}_{ldr}) \quad (6)$$

$$\mathbf{T}_{frld} = AL_{ldr}^{-3} \mathbf{M}_{frm} \times \mathbf{M}_{ldm} + 3AL_{ldr}^{-5} \mathbf{M}_{ldm} \times \mathbf{L}_{ldr} (\mathbf{M}_{frm} \cdot \mathbf{L}_{ldr}) \quad (7)$$

where \mathbf{M}_{frm} is the magnetization of the releasing magnet in the follower robot module and \mathbf{L}_{ldr} represents the distance between the driving magnet in the leader robot module and the releasing magnet in the follower robot module.

Similarly, the releasing magnet in the follower robot module will be applied with propulsive torque by the rotating magnetic

field (\mathbf{T}_{frm}), resistance torque produced by the interaction between the driving magnet in the leader robot module and the releasing magnet in the follower robot module (\mathbf{T}_{ldr}), resistance torque generated by the interaction between the driving magnet in the follower robot module and the releasing magnet in the follower robot module (\mathbf{T}_{fdfr}), and resistance torque produced by the film and friction. The relations between them and the calculation equations can be written as

$$\mathbf{T}_{fr} = \mathbf{T}_{frm} - \mathbf{T}_{ldr} - \mathbf{T}_{fdfr} - \mathbf{T}_{lf} - \mathbf{T}_{ff} \quad (8)$$

$$\mathbf{T}_{frm} = V_{frm} \mathbf{M}_{frm} \times \mathbf{B}_{frm} \quad (9)$$

$$\mathbf{T}_{ldr} = AL_{ldr}^{-3} \mathbf{M}_{ldm} \times \mathbf{M}_{frm} + 3AL_{ldr}^{-5} \mathbf{M}_{frm} \times \mathbf{L}_{ldr} (\mathbf{M}_{ldm} \cdot \mathbf{L}_{ldr}) \quad (10)$$

$$\mathbf{T}_{fdfr} = AL_{fdfr}^{-3} \mathbf{M}_{fdm} \times \mathbf{M}_{frm} + 3AL_{fdfr}^{-5} \mathbf{M}_{frm} \times \mathbf{L}_{fdfr} (\mathbf{M}_{fdm} \cdot \mathbf{L}_{fdfr}) \quad (11)$$

where V_{frm} is the volume of the releasing magnet in the follower robot module, \mathbf{M}_{fdm} is the magnetization of the driving magnet in the follower robot module, and \mathbf{B}_{frm} means the magnetic flux density of the rotating magnetic field applied to the releasing magnet in the follower robot module. The resultant torques applied to the other driving/releasing magnets can be calculated by similar analyses and equations presented above.

During the drug release, the releasing magnet rotates from a static status with the rotation of the rotating magnetic field, and it will have the same rotational speed as the rotating magnetic field after acceleration. Then, the switching baffle rotates to the required positions with the rotating magnetic field. The parameters during the acceleration can be calculated by

$$\begin{bmatrix} \alpha_{dr} \\ \omega_{dr} \cdot \omega_{dr} \end{bmatrix} = \begin{bmatrix} \frac{1}{J_{dr}} \mathbf{T}_{dr} \\ 2\theta_{dr} \cdot \alpha_{dr} \end{bmatrix} \quad (12)$$

where α_{dr} indicates the angular acceleration of the drug release mechanism, J_r is the equivalent moment of inertia of the drug release mechanism, ω_{dr} is the angular velocity of the drug release mechanism, θ_{dr} is the rotation angle of the switching baffle, and \mathbf{T}_{dr} means the resultant torque applied to the releasing magnet. \mathbf{T}_{dr} is the torque calculated through (1) or (8). As for the locomotion of the robot modules, the viscosities and rotational speeds of the robot modules can be obtained by substituting the resultant torques applied to the driving magnet calculated above into our previous calculations in [21].

E. Prototype

The multidrug modular capsule robots were fabricated through 3D printing and assembled in the laboratory. Fig. 6(a) shows three selected types of multidrug modular capsule robots. The leader robot module has dimensions of $\Phi 17 \times 35.2$ mm and all the follower robot modules have the same dimensions of $\Phi 17 \times 39.5$ mm. All the multidrug modular capsule robots employ the same driving magnets and releasing magnets. A cylindrical magnet (NO260, NeoMag, JP) is used as the driving magnet, while the other magnet (NOR047, NeoMag, JP) works as the releasing magnet. The dimensions

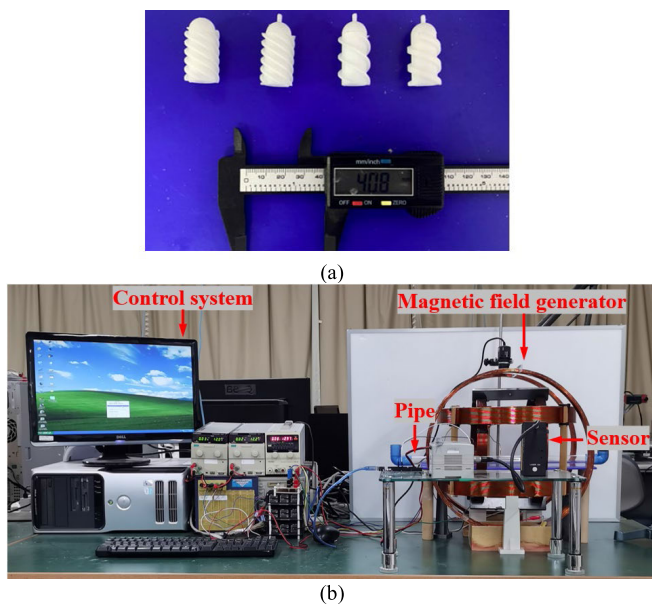


Fig. 6. (a) Assembled multidrug modular capsule robots. (b) Robot system platform.

could be further optimized based on clinical requirements and the types of magnets would be changed accordingly. The generated torques for the driving magnet or releasing magnet can be adjusted by changing the magnetic flux density of the rotating magnetic field and thus the required torques for robot motion or drug release will be obtained when the magnetization of the driving magnet changes with the replacement of different types of magnets. The leader robot module moves at the forefront, so it can be combined with any follower robot modules; each follower robot module can be combined with each other because they have a common combination mechanism.

Fig. 6(b) shows the robot system platform. The platform consists of a control system and a magnetic field generator. The multidrug modular capsule robots are located in the magnetic field generator and can be controlled by the magnetic field generator. The magnetic field generator comprises two sets of x -directional Helmholtz coils, y -directional Helmholtz coils, and z -directional Helmholtz coils, and can generate various magnetic fields. The control information can be input through the control system and can be transferred to voltage signals. With these voltage signals, the magnetic field generator produces specific rotating magnetic fields, and then the required motion of the robot modules will be achieved.

III. PERFORMANCE TEST

In order to test the performance of the multidrug modular capsule robots, experiments were carried out according to the application requirements. Three types of experiments were conducted and they are locomotion experiments, docking and separation experiments, and drug release control experiments.

A. Locomotion Experiments

1) *Experimental Setup:* When multidrug modular capsule robots move in the intestine, they are controlled separately by

the magnetic field generator. Each robot module will have various moving velocities. The moving velocity directly concerns the detection efficiency and interaction/duration of drugs. Thus velocity is a vital factor that should be considered in robot-assisted endoscopy. For example, common commercial capsule robots passively move in the intestinal tract by peristalsis and contractions of the intestine, and they have a long operating time and a low detection efficiency due to the lack of speed control. Thus in these experiments, the moving velocities of the multidrug modular capsule robots with various drug loadings were tested. The experimental setup is also shown in Fig. 6(b). Robot modules were in a pipe with an internal diameter of 20 mm and located in the magnetic field generator. A laser displacement sensor (LK-500, KEYENCE, JP) was used to record the movement time. The robot module moved from the starting point and the displacement sensor was set in the stopping point. The magnetic field generator and the displacement sensor started to work simultaneously. When the data recorded by the displacement sensor change, the recording time is the movement time of the robot modules. The velocities of the robot modules can be calculated through the movement time and distance between the starting point and the stopping point. During these experiments, the multidrug modular capsule robot loaded different loadings. The multidrug modular capsule robot can load up to 1.8 g of drugs and thus the drug weights were set as 0, 0.6, 1.2, and 1.8 g. The magnetic frequency for every single movement was set as 0.5 Hz with 0.5-Hz increment over a range of 10 Hz, and each moving velocity of the multidrug modular capsule robot with the corresponding magnetic frequency was calculated. Each measurement was carried out with ten cycles of repetition.

2) *Experimental Results and Discussion:* One leader robot module and two types of follower robot modules were tested in these experiments, and in order to facilitate the expression of each robot, these three robot modules were named MMCR-A, MMCR-B, and MMCR-C. Fig. 7 shows the velocities of the robot modules with various loads and magnetic frequencies. The maximum advance velocities of the MMCR-A loading drugs of 0, 0.6, 1.2, and 1.8 g are 28.5, 25.1, 22.3, and 14.5 mm/s, respectively. The maximum retreat velocities of the MMCR-A loading drugs of 0, 0.6, 1.2, and 1.8 g are 25.4, 22.1, 19.6, and 11.7 mm/s, respectively. It can be found that the MMCR-A has great velocities when magnetic fields with larger frequencies are applied. This is mainly because magnetic fields with larger frequencies produce great rotary velocities that result in more significant moving velocities. However, this trend of velocity increase with magnetic frequency growth is effective in a certain range. The MMCR-A has a step-out frequency and it cannot start to rotate when the magnetic frequency is larger than this frequency. As shown in Fig. 7(a) and (b), the advance and retreat velocity of the MMCR-A with a drug of 0, 0.6, and 1.2 g is 0 when the magnetic frequency is 4.5 Hz; the advance and retreat velocity of the MMCR-A with a drug of 1.8 g is 0 when the magnetic frequency is 4 Hz. It is due to the fact that the step-out frequency of the MMCR-A with a load of less than 1.2 g drug is 4.5 Hz, and the step-out frequency of the MMCR-A with a load of 1.8 g drug is 4 Hz.

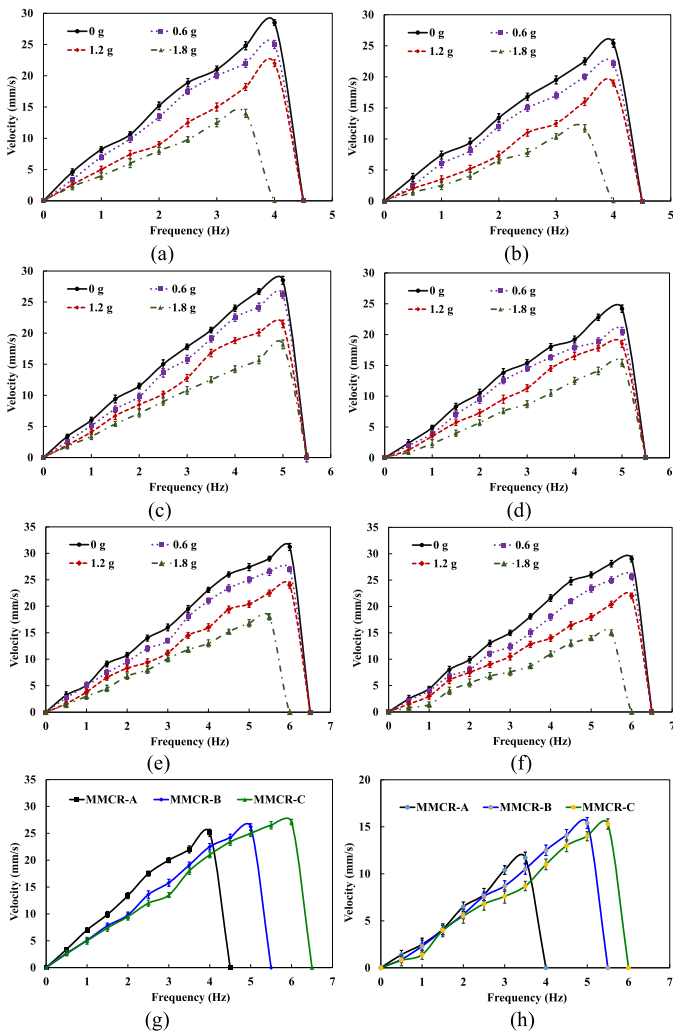


Fig. 7. Moving velocities of robot modules with various loads and magnetic frequencies. (a) MMCR-A moving forward. (b) MMCR-A moving backward. (c) MMCR-B moving forward. (d) MMCR-B moving backward. (e) MMCR-C moving forward. (f) MMCR-C moving backward. (g) Three robot modules moving forward when loading 0.6 g. (h) Three robot modules moving backward when loading 1.8 g.

The MMCR-B and MMCR-C have similar performance to the MMCR-A, and as shown in Fig. 7(c)–(f), the step-out frequency of the MMCR-B is 5.5 Hz; the step-out frequency of the MMCR-C with a load less than 1.2 g drug is 6.5 Hz and the step-out frequency of the MMCR-C with a load of 1.8 g drug is 6 Hz. The experimental results show that multidrug modular capsule robots can be controlled separately by using a magnetic field with different driving frequencies since they have various step-out frequencies. In addition, it can also be found that each robot module has different velocities when it moves forward and backward. This is mainly because the structures of the thread mechanism, claw mechanism, and drug release mechanism differ from each and these different structures will result in various moving resistances. In addition, to comprehensively evaluate the locomotion/loading performance of the robot modules, we compared the velocities of the three robot modules with the same load. Fig. 7(g) and (h) shows the velocities of the robot modules loading drugs of 0.6 g when moved forward and loading drugs of 1.8 g when

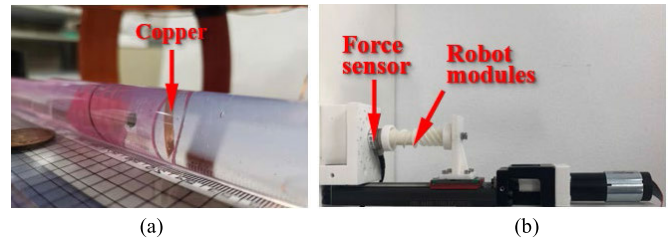


Fig. 8. Setup for the docking and separation experiments. (a) Measuring the propulsive force. (b) Measuring the required forces and torque for docking and separation.

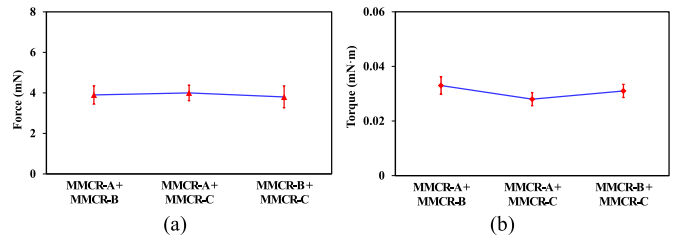


Fig. 9. Required force and torque for docking and separation. (a) Force for docking. (b) Torque for separation.

moved backward, respectively. The three curves have a similar tendency, demonstrating the similar locomotion and loading ability of the three robot modules.

B. Docking and Separation Experiments

1) *Experimental Setup*: When multidrug modular capsule robots are used to perform diagnosis and treatment, they need to dock and separate from each other. To test whether they are able to dock and separate from each other successfully during the procedures, experiments were carried out to test their docking and separation performance. To measure the propulsive forces of the multidrug modular capsule robots, we set a sheet of copper in the pipe and calculated the propulsive forces based on the deformation of the copper. The experimental setup is shown in Fig. 8(a). Since we cannot directly measure the propulsive torques of the multidrug modular capsule robots without introducing an effect on the robot movement, we obtained the propulsive torques based on the movement videos. The robot module started to rotate from the static state, then gradually accelerated, and finally rotated at a uniform speed. The rotational speed and time were obtained by the video, and thus the propulsive torque was calculated by using this movement information and the moment of inertia of the robot module.

In order to measure the required forces and torque for docking and separation, an ATI force sensor was used and mounted on a plate. As shown in Fig. 8(b), when the motor drove the slider to move, two robot modules achieved docking and the maximum force during the process was the required force for docking. These two robot modules rotated in opposite directions to realize separation and the torques during the procedure were measured by the ATI force sensor. The maximum torque was the required torque for separation. Ten cycles of repetition were carried out for each measurement in the docking and separation experiments.

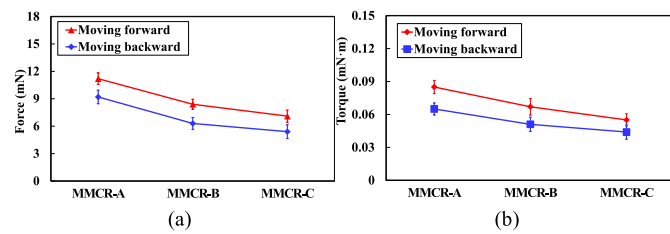


Fig. 10. Propulsive forces and torques of robot modules. (a) Forces. (b) Torques.

2) *Experimental Results and Discussion*: Fig. 9 shows the required force and torque for docking and separation. The maximal required forces for docking between MMCR-A and MMCR-B, MMCR-A and MMCR-C, and MMCR-B and MMCR-C, are 3.9, 4.0, and 3.8 mN, respectively. The maximal required torques for separation between MMCR-A and MMCR-B, MMCR-A and MMCR-C, and MMCR-B and MMCR-C, are 0.033, 0.028, and 0.031 mN · m, respectively. Fig. 10 shows the propulsive forces and torques of the multidrug modular capsule robots. The average minimal propulsive forces of MMCR-A, MMCR-B, and MMCR-C are 11.2, 8.4, and 7.1 mN, respectively, when they move forward. When they move backward, the average minimal propulsive forces of MMCR-A, MMCR-B, and MMCR-C are 9.2, 6.3, and 5.4 mN, respectively. The average minimal propulsive torques of MMCR-A, MMCR-B, and MMCR-C are 0.085, 0.067, and 0.055 mN · m, respectively when they move forward. When they move backward, the average minimal propulsive torques of MMCR-A, MMCR-B, and MMCR-C are 0.065, 0.051, and 0.044 mN · m, respectively. Every multidrug modular capsule robot has different propulsive forces and torques when moving forward and backward.

As discussed in Section III-A2, the multidrug modular capsule robots have different structures on their front and back ends and thus they possess various propulsive forces and torques when moving forward and backward. Comparing the average minimal propulsive forces with the required forces for docking, it is found that the multidrug modular capsule robots can produce larger propulsive forces than the required forces for docking, and thus the multidrug modular capsule robots can dock with each other using the propulsive forces. Similarly, the multidrug modular capsule robots will generate larger propulsive torques than the required torques for separation and this means that they can achieve separation with the propulsive torques.

C. Drug Release Control Experiments

1) *Experimental Setup*: The multidrug modular capsule robots carry various drugs to the target positions and release the drugs according to the clinical requirements. To test whether the multidrug modular capsule robots can release the drugs with the orders, drug release experiments were carried out. In these experiments, the multidrug modular capsule robots were located in the magnetic field generator and can be controlled by the magnetic field generator. The magnetic field generator produces magnetic fields to the drug release mechanism of the multidrug modular capsule robots. The

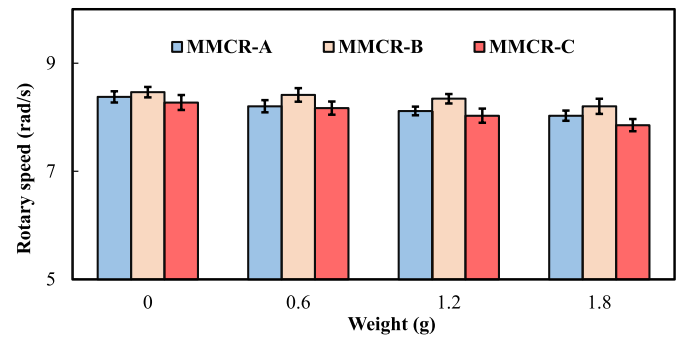


Fig. 11. Rotary speeds of the rotating baffle of multifunctional modular capsule robots A, B, and C with various drug loadings.

drug release mechanism has two limited positions, and the switching baffle can move between them. For the multidrug modular capsule robots, the angle formed by these two extreme positions is 75° . The switching baffle was positioned at one position and rotated to the other position by the rotation of the magnetic fields. To test the effect of the drug weight on the rotation of the switching baffle, the switching baffle was rotated with different weights of drugs. The magnetic frequency was set as 1.5 Hz. The weight of the loaded drug for each experiment was set as 0, 0.6, 1.2, and 1.8 g since the maximum drug loading capacity of the MCR is 1.8 g. The rotary time was recorded and then the rotary speed was calculated. Every measurement was repeated ten times and the standard deviations were calculated.

2) *Experimental Results and Discussion*: The rotary speeds of the switching baffle of multidrug modular capsule robots with various drug loadings are shown in Fig. 11. The average rotary speeds of the switching baffle of MMCR-A are 8.37, 8.20, 8.11, and 8.02 rad/s when the weights of the loaded drugs are 0, 0.6, 1.2, and 1.8 g, respectively. The switching baffle of MMCR-A had a maximum rotary speed when MMCR-A loaded drugs of 0 g. The switching baffle of MMCR-A had a minimum rotary speed when MMCR-A loaded drugs of 1.8 g. Drug weight affects the rotary speed of the switching baffle. The loaded drug exerts pressure on the switching baffle, and this pressure impedes the rotation of the switching baffle. Therefore, great drug weight results in lower rotary speed. Similarly, the average rotary speeds of the switching baffle of MMCR-B are 8.46, 8.41, 8.34, and 8.20 rad/s when the weights of the loaded drugs are 0, 0.6, 1.2, and 1.8 g, respectively. The average rotary speeds of the switching baffle of MMCR-C are 8.27, 8.16, 8.03, and 7.85 rad/s when the weights of the loaded drugs are 0, 0.6, 1.2, and 1.8 g, respectively. MMCR-B and MMCR-C have the same rotary speed change trends and reasons as MMCR-A.

When MMCR-A is fully loaded with drugs of 1.8 g, the rotary speed is 8.02 rad/s. Thus, MMCR-A can open the switching baffle for drug release in 0.028 s. Similarly, the minimum rotary speeds of MMCR-B and MMCR-C are 8.20 and 7.85 rad/s, respectively, when they are fully loaded, and they can open the switching baffle for drug release within 0.03 s. This means that the switching baffle can be opened instantly, and therefore, these rotary speeds would be acceptable for drug release.

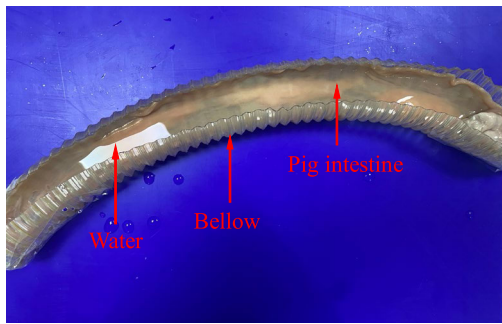


Fig. 12. Experimental setup for ex vivo experiments.

IV. EX VIVO EXPERIMENTS

A. Experimental Setup

To test the feasibility of the actual application of the multidrug modular capsule robots, ex vivo experiments were carried out. A pig intestine was used to simulate the human intestine. The pig intestine was acquired from a food supplier and there is no ethics required. As shown in Fig. 12, the intestine was dissected and set in a flexible bellow. There is a small amount of water in the small intestine to simulate the intestinal environment. First, in experiment I, one multidrug modular capsule robot was used and it was located in the intestine. The intestine was located in the magnetic field generator, and thus, the multidrug modular capsule robot could be controlled by the magnetic field generator. The experimental setup is the same as that in Section III-A. MMCR-A was used in this experiment, and two types of water, dyed blue and black, used to replace drugs A and B, were injected into compartments A and B of MMCR-A, respectively. The magnetic field generator was used to produce magnetic fields in various directions to realize different functions of MMCR-A. A rotating magnetic field of 3 Hz was generated first to rotate the main body of the MMCR-A and then the MMCR-A moved forward. When MMCR-A moved to target A [targets A and B are shown in Fig. 13(a)], it stopped and a constant magnetic field was then generated to adjust the pose of MMCR-A. With a rotating magnetic field of 1.5 Hz, the switching baffle started to rotate. Drug A was released at target A. Then, the rotating magnetic field of 3 Hz was generated again to rotate MMCR-A. Similarly, MMCR-A moved to target B and released drug B. All the entire movements were videotaped by a camera. Two areas of the intestinal wall, located on the movement path and drug release position, were selected for observation.

In experiment II, both MMCR-A and MMCR-B were used, and they tried to dock and separate with each and release different drugs. The black and red water used to replace drugs A and B were injected into compartments A and B of MMCR-A, respectively. Similarly, blue and red water was injected into compartment A and compartment of MMCR-B to release drugs C and D. MMCR-A and MMCR-B were set in the intestine and the magnetic field generator started to generate different types of magnetic fields. The rotating magnetic fields of 3 Hz drove MMCR-A to move forward and reach target A [targets A and B are shown in Fig. 13(a)]. After MMCR-A stopped at target A, a constant magnetic field was generated to adjust the pose of MMCR-A then a rotating magnetic field of 1.5 Hz to release drug A. Next, the rotating magnetic

fields of 5 Hz drove MMCR-B to move forward and dock with MMCR-A, and then the docked MMCR-A and MMCR-B moved together with the rotating magnetic. When they reached target B, MMCR-A released drug B and MMCR-B released drug C. After the drug release, MMCR-A and MMCR-B were separated and then moved forward. During this procedure, all the operations were photographed. Three areas of the intestinal wall, located on the movement path and drug release position, were selected for observation.

B. Experimental Results and Discussion

The movement and drug release process of the multidrug modular capsule robot in experiment I are shown in Fig. 13. MMCR-A started to move from the original position and toward target A [see Fig. 13(a)] and then rotated the switching baffle clockwise and released drug A [red water in Fig. 13(b)]. After the drug release, MMCR-A rotated its main body and moved forward, stopped at target B rotated the switching baffle counterclockwise and released drug B [blue water in Fig. 13(c)]. After releasing drug B, MMCR-A continued to move forward. The lining of the intestine was photographed before and after experiments. The photographs of the selected areas are shown in Fig. 14. The intestinal wall in Fig. 14(c) and (d) was dyed since drugs were released near this position. With the comparison of these photographs, no noticeable difference was observed by the naked eye.

Fig. 15 shows the procedures of the dock, separation, and multidrug release of two multidrug modular capsule robots in experiment II. As shown in Fig. 15(a), MMCR-A and MMCR-B were located in the original position, and MMCR-A would rotate with the rotating magnetic fields. MMCR-A moved to target A and stopped and then rotated the switching baffle to release drug A [see Fig. 15(b)]. Then, MMCR-B moved toward MMCR-A and docked with MMCR-A [see Fig. 15(c)]. When the docked MMCR-A and MMCR-B moved to target B, they stopped; MMCR-A rotated its switching baffle to release drug B, and MMCR-B rotated its switching baffle to release drug C [see Fig. 15(d)]. Then, MMCR-A and MMCR-B were separated and continued to move forward [see Fig. 15(e)]. The intestinal wall was also observed before and after experiments. Fig. 16 shows the photographed lining of the intestine before and after experiments. The intestinal wall in Fig. 16(c) and (d) was also dyed since drugs were released near this position. With the comparison of these photographs, no noticeable difference was observed by the naked eye.

Experiment I showed that the multidrug modular capsule robot has the ability to load two types of drugs, move to different targets, and release selected drugs at desired positions. Experiment II demonstrated that two multidrug modular capsule robots can cooperate with each other through docking and separation and release multidrugs at desired positions. For the observation of the photographed lining of the intestine before and after experiments in experiments I and II, the “no noticeable difference” could not strictly demonstrate that the multidrug modular capsule robot produces no injuries to the intestine. Specific injury assessment requires professional medical assessment, especially microscopes. The professional medical assessment was not performed currently, but this

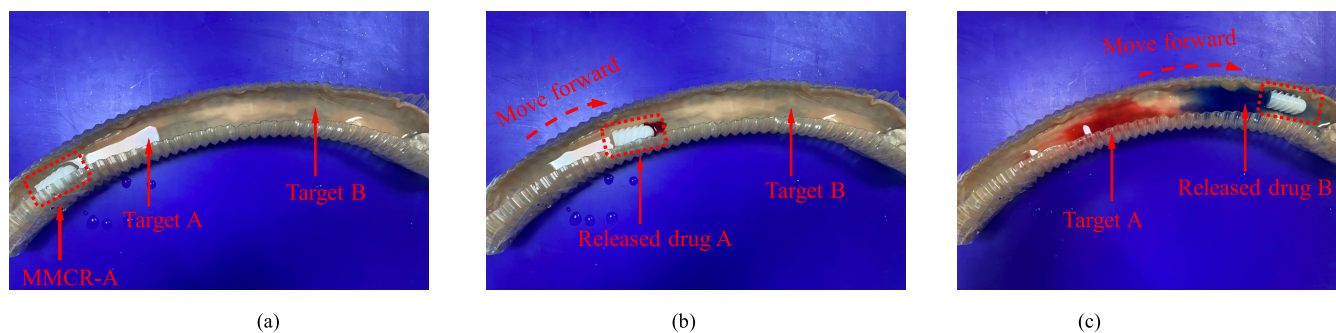


Fig. 13. Locomotion and drug release process in experiment I. (a)–(c) Record pictures during operation.

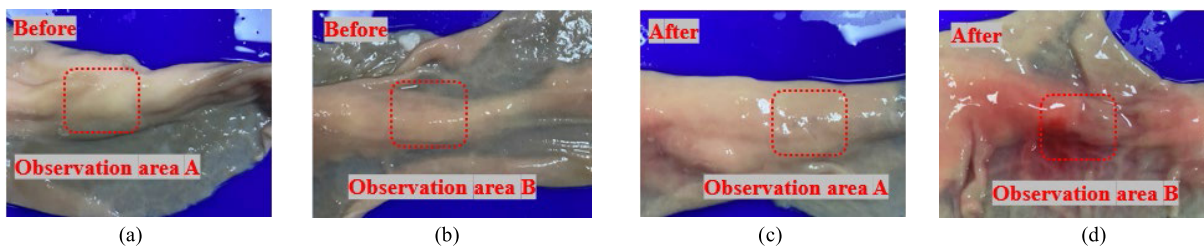


Fig. 14. Observation areas photographed before and after experiments in experiment I (a) and (b) before experiments and (c) and (d) after experiments.

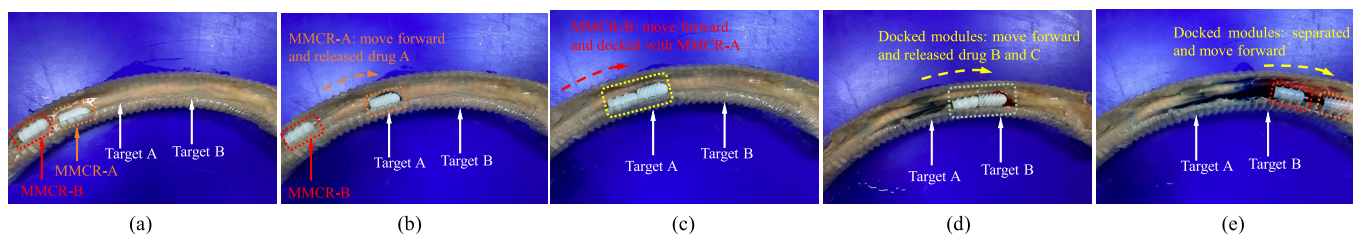


Fig. 15. Locomotion, docking, separation, and multidrug release process in experiment II. (a)–(e) Record pictures during operation.

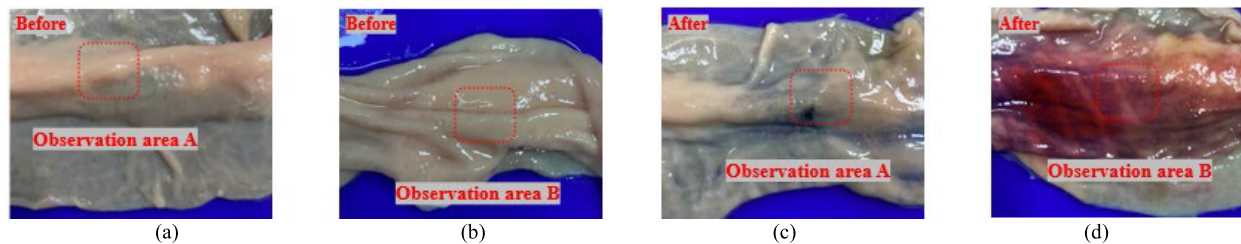


Fig. 16. Observation areas photographed before and after experiments in experiment II (a) and (b) before experiments and (c) and (d) after experiments.

elementary assessment using naked eye observation can preliminarily show the injury level of the multidrug modular capsule robot to the intestine. The worst situation for this “no noticeable difference” is a slight injury to the intestinal wall. Since this kind of injury is not visible to the naked eye, this possible slight injury would not seriously affect the patients’ rehabilitation or operation safety. In addition, in these experiments, the multidrug modular capsule robot was fabricated through 3D printing and the spiral wings on the surface of the multidrug modular capsule robot have a high hardness that might scratch the intestinal wall. In future applications, soft materials will be employed to fabricate the spiral wings, which can not only further reduce injuries to the intestine but also facilitate the swallowing of patients. These

operation processes conducted in experiments I and II did not represent any treatment process or method but were used to test the feasibility of the operation. This proposed multidrug modular capsule robot would have potential applications.

V. CONCLUSION

In this article, we proposed a multidrug modular capsule robot system and verified its performance through laboratory experiments and ex vivo experiments. Experimental results demonstrated that the proposed multidrug modular capsule robot could release multiple drugs, perform docking and separation, and did not cause damage to the lining of the intestine. This proposed multidrug modular capsule robot could prove a reference for drug release and control and have the potential

for further applications. However, several limitations still exist in this research. First, the robot modules were fabricated through 3-D printing and they cannot be used clinically. Second, we did not integrate the camera into the leader robot module and instead used a drug release mechanism since we have not conducted the wireless power supply technology. Third, the pig intestine used in the ex vivo experiments can well simulate the human intestine but there are still some differences. In the future study, we will overcome these limitations and try to conduct animal experiments.

REFERENCES

- [1] I. Peate, "The gastrointestinal system," *Brit. J. Healthcare Assistants*, vol. 15, no. 3, pp. 132–137, 2021.
- [2] M. Singh, S. U. Kafle, N. Kafle, A. Sinha, and P. Rajbhandari, "Histopathological distribution of the gastrointestinal tract lesions," *Birat J. Health Sci.*, vol. 6, no. 2, pp. 1529–1534, Nov. 2021.
- [3] N. Manabe, S. Tanaka, A. Fukumoto, M. Nakao, D. Kamino, and K. Chayama, "Double-balloon enteroscopy in patients with GI bleeding of obscure origin," *Gastrointestinal Endoscopy*, vol. 64, no. 1, pp. 135–140, Jul. 2006.
- [4] X.-B. Li et al., "The role of capsule endoscopy combined with double-balloon enteroscopy in diagnosis of small bowel diseases," *Chin. Med. J.*, vol. 120, no. 1, pp. 30–35, Jan. 2007.
- [5] E. Rondonotti, F. Villa, C. J. J. Mulder, M. A. J. M. Jacobs, and R. de Franchis, "Small bowel capsule endoscopy in 2007: Indications, risks and limitations," *World J. Gastroenterol.*, vol. 13, no. 46, pp. 6140–6149, 2007.
- [6] S. S. Mapara and V. B. Patravale, "Medical capsule robots: A renaissance for diagnostics, drug delivery and surgical treatment," *J. Controlled Release*, vol. 261, pp. 337–351, Sep. 2017.
- [7] H. Zhou and G. Alici, "A novel magnetic anchoring system for wireless capsule endoscopes operating within the gastrointestinal tract," *IEEE/ASME Trans. Mechatronics*, vol. 24, no. 3, pp. 1106–1116, Jun. 2019.
- [8] S. H. Kim and H. J. Chun, "Capsule endoscopy: Pitfalls and approaches to overcome," *Diagnostics*, vol. 11, no. 10, p. 1765, Sep. 2021.
- [9] J. Min, Y. Yang, Z. Wu, and W. Gao, "Robotics in the gut," *Adv. Therapeutics*, vol. 3, no. 4, Apr. 2020, Art. no. 1900125.
- [10] Y.-L. Liu, D. Chen, P. Shang, and D.-C. Yin, "A review of magnet systems for targeted drug delivery," *J. Controlled Release*, vol. 302, pp. 90–104, May 2019.
- [11] F. Munoz, G. Alici, and W. Li, "A review of drug delivery systems for capsule endoscopy," *Adv. Drug Del. Rev.*, vol. 71, pp. 77–85, May 2014.
- [12] J. Nam, W. Lee, J. Kim, and G. Jang, "Magnetic helical robot for targeted drug-delivery in tubular environments," *IEEE/ASME Trans. Mechatronics*, vol. 22, no. 6, pp. 2461–2468, Dec. 2017.
- [13] F. Munoz, G. Alici, H. Zhou, W. Li, and M. Sitti, "Analysis of magnetic interaction in remotely controlled magnetic devices and its application to a capsule robot for drug delivery," *IEEE/ASME Trans. Mechatronics*, vol. 23, no. 1, pp. 298–310, Feb. 2018.
- [14] K. T. Nguyen, M. C. Hoang, E. Choi, B. Kang, J.-O. Park, and C.-S. Kim, "Medical microrobot—A drug delivery capsule endoscope with active locomotion and drug release mechanism: Proof of concept," *Int. J. Control, Autom. Syst.*, vol. 18, no. 1, pp. 65–75, Jan. 2020.
- [15] S. Song et al., "Integrated design and decoupled control of anchoring and drug release for wireless capsule robots," *IEEE/ASME Trans. Mechatronics*, vol. 27, no. 5, pp. 2897–2907, Oct. 2022.
- [16] J. Guo, Z. Bao, S. Guo, and Q. Fu, "Design and evaluation of a new push-type targeted drug delivery capsule robot," in *Proc. IEEE Int. Conf. Mechatronics Autom. (ICMA)*, Tianjin, China, Aug. 2019, pp. 1305–1310.
- [17] S. Guo, Y. Hu, J. Guo, and Q. Fu, "Design of a novel drug-delivery capsule robot," in *Proc. IEEE Int. Conf. Mechatronics Autom. (ICMA)*, Takamatsu, Japan, Aug. 2021, pp. 938–943.
- [18] Z. Wang, S. Guo, J. Guo, Q. Fu, L. Zheng, and T. Tamiya, "Selective motion control of a novel magnetic-driven microbot with targeted drug sustained-release function," *IEEE/ASME Trans. Mechatronics*, vol. 27, no. 1, pp. 336–347, Feb. 2022.
- [19] Z. Wang, S. Guo, and W. Wei, "Modeling and simulation of the drug delivery function for a magnetic driven capsule robot," in *Proc. IEEE Int. Conf. Mechatronics Autom. (ICMA)*, Beijing, China, Oct. 2020, pp. 1384–1388.
- [20] L. Zheng, S. Guo, and M. Kawanishi, "Magnetically controlled multi-functional capsule robot for dual-drug delivery," *IEEE Syst. J.*, vol. 16, no. 4, pp. 6413–6424, Dec. 2022.
- [21] S. Guo, Q. Yang, L. Bai, and Y. Zhao, "Development of multiple capsule robots in pipe," *Micromachines*, vol. 9, no. 6, pp. 147–152, 2018.
- [22] L. Zheng, S. Guo, Z. Wang, and T. Tamiya, "A multi-functional module-based capsule robot," *IEEE Sensors J.*, vol. 21, no. 10, pp. 12057–12067, May 2021.



Lingling Zheng received the Ph.D. degree in intelligent mechanical systems engineering from the Faculty of Engineering and Design, Kagawa University, Takamatsu, Japan, in 2022.

She is currently an Assistant Professor at the School of Information Engineering and the School of Artificial Intelligence, Nanjing Xiaozhuang University, Nanjing, China. Her current research interests include medical robots and microrobots.



Shuxiang Guo (Fellow, IEEE) received the Ph.D. degree in mechatronics and systems from Nagoya University, Nagoya, Japan, in 1995.

He is currently a Chair Professor with the Department of Electronic and Electrical Engineering, Southern University of Science and Technology, Shenzhen, China, and a Chair Professor with the Key Laboratory of Convergence Medical Engineering System and Healthcare Technology, Ministry of Industry and Information

Technology, Beijing Institute of Technology, Beijing, China. His research interests include medical robot systems, microcatheter systems, and biomimetic underwater robots.

Dr. Guo is a Fellow of The Engineering Academy of Japan.



Masahiko Kawanishi (Member, IEEE) received the B.S. degree from the Faculty of Medicine, Kagawa Medical University, Takamatsu, Japan, in 1993.

He is currently an Associate Professor with the Faculty of Medicine, Kagawa University, Takamatsu. His current research includes the surgical techniques of neurosurgical operations and intravascular surgery systems.